Heliyon

Received:
21 January 2019
Revised:
8 March 2019
Accepted:
21 March 2019

Cite as: Kiplangat Rop, Damaris Mbui, Njagi Njomo, George N. Karuku, Immaculate Michira, Rachel F. Ajayi. Biodegradable water hyacinth cellulose-graft-poly(ammonium acrylate-co-acrylic acid) polymer hydrogel for potential agricultural application. Heliyon 5 (2019) e01416. doi: 10.1016/j.heliyon.2019.e01416

Biodegradable water hyacinth cellulose-graft-poly(ammonium acrylate-co-acrylic acid) polymer hydrogel for potential agricultural application

Kiplangat Rop [a,*], **Damaris Mbui** [a], **Njagi Njomo** [a], **George N. Karuku** [b], **Immaculate Michira** [a], **Rachel F. Ajayi** [c]

[a] *Department of Chemistry, University of Nairobi, P.O. Box 30197-00100, Nairobi, Kenya*

[b] *Department of Land Resource Management and Agricultural Technology, University of Nairobi, P. O. Box 29053-00625, Kangemi, Nairobi, Kenya*

[c] *Department of Chemistry, University of the Western Cape, Private Bag X17, Bellville, 7535, South Africa*

[*] Corresponding author.

E-mail addresses: kiplangatrop@gmail.com, kiplangatrop@uonbi.ac.ke (K. Rop).

Abstract

Swollen cellulose fibres isolated from water hyacinth were utilized in the synthesis of water hyacinth cellulose-graft-poly(ammonium acrylate-co-acrylic acid) polymer hydrogel (PHG). Acrylic acid (AA) partially neutralized with NH_3 was heterogeneously grafted onto swollen cellulose by radical polymerization reaction using *N,N*-methylene-*bis*-acrylamide (MBA) as the cross-linker and ammonium persulphate (APS) as the initiator. The reaction conditions were optimized through assessment of grafting parameters such as grafting cross-linking percentage (GCP), percentage grafting cross-linking efficiency (%GCE) and water absorption tests. Characterization of the copolymer by Fourier Transform Infra-red (FTIR) spectroscopy revealed successful grafting of the monomer onto cellulose. Transmission electron microscopy (TEM) image of acetone-extracted PHG displayed micro-porous structure. The optimized product swelled in distilled water up to 165 times its own dry weight. The swelling was influenced by the pH and presence, nature and concentration of ions. The hydrogel had the

https://doi.org/10.1016/j.heliyon.2019.e01416

capacity to retain moisture in soil, and degradation testing revealed a higher mass loss in cellulose grafted copolymer compared to the copolymer without cellulose. Degradation by soil microbial isolates showed significantly higher ($P \leq 0.05$) accumulation of NH_4^+ in the cellulose grafted copolymer up to 0.05% (w/v) from 40 to 100 h, relative to similar amounts of copolymer without cellulose. The use of water hyacinth, a notorious weed in Kenyan waters, to produce cellulose-based polymer hydrogels has not been explored and yet, it could form an effective and beneficial way of utilizing this plant. A mechanism of graft polymerization reaction has also been proposed. The synthesized product can be applied in agriculture and other fields where biodegradability and effective utilization of water is essential.

Keyword: Materials science

1. Introduction

Polymer hydrogels (PHGs) are three-dimensional network hydrophilic materials with a capacity to swell in water and maintain the swollen state, even under pressure. PHGs with high absorption capacities of up to 1000 times their own dry weight are called superabsorbent polymers (SAPs) [1, 2, 3, 4]. The ability to absorb and retain water is attributed to hydrophilic groups such as -OH, -CONH-, $-CONH_2$ and $-SO_3H$, while resistance to dissolution is attributed to cross-links between polymer chains [1, 2, 3]. SAPs have wide applications in food industry, pharmaceuticals, agriculture, bio-medicine, bio-engineering and environmental remediation, among others [1, 3, 4].

Depending on the source, hydrogels are often divided into synthetic and natural hydrogels. Synthetic PHGs have excellent water absorbency, long shelf lives and high gel strength [1, 2]. However, non-biodegradability and toxicity in the environment limit their use in agriculture and consumer products [2]. For this reason, eco-friendly and sustainable bio-based products are being investigated due to increased environmental consciousness. Natural-based PHGs have been developed by amalgamating synthetic and natural substrates such as polysaccharides and polypeptides [1]. Polysaccharides have attracted much attention and cellulose being one of them, is rated as the best potential candidate for the production of bio-based PHGs due to its properties such as biodegradability, biocompatibility, hydrophilicity and good mechanical strength, among others [4]. Cellulose is an active biopolymer due to the presence of three -OH groups in each of its *D*-anhydroglucopyranose units, and chemical modifications can be performed on them. The primary -OH at C-6 and two secondary ones at C-2 and C-3 can participate in classical reactions such as esterification, etherification and oxidation [5, 6, 7]. Cellulose derivatives have been obtained by reacting some (or all) −OH groups of cellulose repeat unit. The

https://doi.org/10.1016/j.heliyon.2019.e01416

most commonly produced cellulose derivatives are cellulose ethers such as ethyl cellulose, carboxymethyl cellulose, hydroxyethyl cellulose, hydroxypropyl cellulose, and cellulose esters such as cellulose acetate and cellulose acetate propionate [8].

Synthesis of graft copolymers is another way in which physical and chemical properties of cellulose can be modified. Grafting of monomers onto cellulose or its derivatives has been performed using techniques such as free radical polymerization (FRP), ring opening polymerization (ROP) and 'living' or controlled radical polymerization (CRP) [5, 8]. The techniques of grafting are based on one (or more) of the three approaches; "grafting to" in which pre-formed polymer with its reactive end-group is coupled with functional groups located on the cellulose backbone, "grafting from" where polymer chains are grown from initiating site on cellulose backbone, or "grafting through" where the substrate bears a polymerizable group, hence acts as a macro-monomer, and polymerization of monomers takes place in the presence of this substrate [5, 8, 9]. FRP is often preferred technique because of relative insensitivity to impurities and moderate reaction conditions. Grafting of vinyl monomers to pre-existing polymeric backbone by FRP mechanism generally involves "grafting from" approach, and radicals are generated using initiation techniques such as UV, high energy irradiation (γ-ray or electron beams) and redox initiation with Mn or Ce (iv) ion, among others [1, 10]. The "grafting from" approach is often preferred because of high grafting density achieved, "grafting to" often suffers from steric hindrance limiting the final grafting density, while "grafting through" is relatively convenient but requires synthesis of cellulose derived macro-monomers [9]. The use of ROP method is limited by demanding experimental conditions such as low temperature, use of high purity reagents, inert atmosphere, anhydrous conditions, and direct use of carbocations that require protection of -OH groups in cellulose to avoid side reactions. The disadvantages of FRP are poor control over composition, architecture and molecular weight distribution. To overcome these drawbacks, CRP techniques such as atom transfer radical polymerization, reversible addition-fragmentation chain transfer polymerization and nitroxide-mediated polymerization have been developed [5].

Cellulose-based hydrogels are commonly synthesized using cellulose derivatives such as carboxymethyl cellulose [12] and sodium carboxymethyl cellulose [13, 14, 15] by FRP technique. Polymerization reactions with these derivatives as substrates are performed under homogeneous reaction mixtures because of their solubility in various solvents. The -OH groups in cellulose chains enable grafting of vinyl monomers enhancing hydrophilicity, a feature useful in application prospects such as agriculture where biodegradability, and water retention and release is essential. Despite exhibiting properties with potential application as fertilizer carriers and soil conditioners, high cost of producing bio-based hydrogels using cellulose derivatives limits their application. However, cellulose being the most abundant and

https://doi.org/10.1016/j.heliyon.2019.e01416

renewable biopolymer, can be derived from a wide variety of biomass such as the water hyacinth (*Eichhornia crassipes*). Activation treatments such as swelling (in acids, bases, etc.) and mechanical pulping, of lignocellulosic material, open the surface cannulae, internal pores and cavities, disrupt fibrillar aggregations and crystalline order, and break inter- and intra-H bonds, enhancing accessibility and reactivity of -OH groups in a heterogeneous chemical reaction [5, 11].

Water hyacinth (WH), an invasive non-native species in Kenya, infests rivers, dams, lakes and irrigation channels, causing serious economic and environmental problems [10, 16]. Due to the hyacinth's high growth rate, it has been a great challenge to control its invasion and proliferation. The use of herbicide to eliminate this weed is effective, but herbicides' effects are hazardous to the environment. Water hyacinth has been utilized locally as compost manure, feed for animals and fish, papermaking, crafts (ropes, baskets, chairs, fibreboards) [16, 17], wastewater treatment [18], production of biogas [19], ethanol [20] and charcoal briquettes [21], among others. However, utilization of WH cellulose in the production of PHG has not been explored. This study aimed at producing biodegradable PHG by heterogeneously grafting acrylic monomers onto cellulose fibres isolated from WH, as an alternative means of managing its invasiveness coupled with economic gain. The use of cellulose derived from WH can reduce the cost of production, impart biodegradability, and enhance the swelling and mechanical strength while at the same time helping to root out the weed.

2. Material and methods

2.1. Materials

Cellulose was extracted from water hyacinth; acrylic acid and *N,N*-methylene−*bis*-acrylamide were obtained from ACROS Organics, Germany. Ammonium persulphate, acetone, toluene, ammonium hydroxide, hydrochloric acid, sulphuric acid, sodium hypochlorite, sodium chloride, calcium chloride and aluminium chloride were obtained from Loba Chemie, Mumbai, India.

2.2. Sample preparation

Fresh water hyacinth (WH) plants were collected from Nairobi dam and then washed with water to remove dirt and any other material attached to the surface. They were then separated into leaves, stems and roots for use during characterization. The plant parts were chopped into small pieces and air-dried in the shade. The particle size of dried material was further reduced through milling to increase its surface area. Samples were stored in air-tight polythene bags ready for use in the experiments.

https://doi.org/10.1016/j.heliyon.2019.e01416

2.3. Characterization of water hyacinth

The characterization method was adopted from Istirokhatun *et al.* [17], Abdel-Halim [22] and Kaco *et al.* [23]. The moisture and ash content of the air-dried WH samples were determined gravimetrically. Hemicellulose was isolated by treating the samples with KOH (10 % w/v) and then precipitating the resulting mixture with ethanol. For lignin content determination, the air-dried WH samples were first treated with toluene/ethanol (2:1). The solvent-extracted samples were treated with 72 % v/v H_2SO_4 at low temperature. The resultant extract was solubilized through heating, and insoluble lignin retained. The cellulose content was determined by subtracting the sum of moisture, ash, hemicellulose and lignin content from 100 %.

2.4. Isolation of cellulose from water hyacinth

Cellulose was isolated from WH according to Istirokhatun *et al.* [17]. Air-dried WH samples were refluxed in a toluene/ethanol solvent mixture (2:1) for 3 h and then allowed to cool to room temperature, after which they were filtered and air-dried. The solvent-extracted samples were bleached using 3 % NaOCl in a water bath at 80 °C for 2 h. Hemicellulose was removed through alkaline hydrolysis using 2 % NaOH at 60 °C for 2 h. Samples were bleached again by heating in 2 % NaOCl with stirring at 75 °C for 3 h. The last stage was acid hydrolysis, using 5 % HCl as the catalyst at 65 °C for 6 h. The isolated cellulose was washed with water and then made alkaline by adding 0.1 M NaOH to avoid microbial degradation over time. The alkaline cellulose was neutralized with 0.1 M HCl and washed with distilled water before use in subsequent experiments.

2.5. Determination of dry weight of cellulose in swollen cellulose fibres

30 mL of swollen cellulose fibres were drawn using a syringe, transferred onto a filter cloth and allowed to drain, then oven-dried at 105 °C to a constant weight. This was replicated three times and the average dry weight value was determined using an analytical balance with a precision of ±0.01 g. The water content in swollen cellulose fibres was maintained through regular repeat of the procedure.

2.6. Synthesis of water hyacinth cellulose-g-poly(ammonium acrylate-co-acrylic acid)

The method followed was adopted from Soleimani and Sadeghi [24]. Swollen cellulose fibres containing 0.6−1.25 g dry weight of cellulose, were transferred using a syringe into a 3-necked flask. The flask was then fitted with a reflux condenser and nitrogen line, and then placed in a temperature-controlled water bath equipped with a magnetic stirrer. Nitrogen gas was bubbled through the mixture for 10 min, as the

https://doi.org/10.1016/j.heliyon.2019.e01416

temperature was gradually raised to 70 °C. Ammonium persulphate (APS) (0.05−0.25 g) was added into the mixture and stirred for 30 min to generate free radicals. Acrylic acid (AA) partially neutralized with NH_3 solution and *N,N*-methylene-*bis*-acrylamide (MBA) were blended, stirred to dissolve and then introduced into the reaction flask. The total volume of the reaction mixture was varied between 40 and 50 mL by adding distilled water after which it was stirred for 1 min and left to stand for 2 h. The PHG formed was allowed to cool to room temperature, removed and then cut into small pieces. These were soaked in distilled water and a 1:1 NH_3 solution was added dropwise to adjust the pH to 8; then washed with water and oven dried at 60 °C to constant weight.

2.6.1. Extraction of homopolymers

A 0.5 g dry PHG sample (particle size $\leq$ 2 mm) was soaked overnight in 100 mL of distilled water in a beaker. It was soxhlet extracted with acetone for 2 h to remove the homopolymers and other impurities. The copolymer obtained was oven dried at 60 °C to a constant weight, pulverized and then kept in air-tight polyethylene bottles for subsequent experiments.

2.6.2. Optimization of reaction conditions

The optimal reaction conditions were obtained by changing one synthetic variable at a time. The synthetic variables included; monomer to cross-linker ratio, degree of neutralization, initiator concentration, cellulose content, total volume of reaction mixture and the reaction temperature. Grafting of the monomer onto cellulose was monitored gravimetrically, where the weight gain in cellulose after extracting the homopolymer was used to determine grafting parameters [14, 25, 26]. It was also taken as a confirmation of successful grafting. The grafting parameters, *i.e.,* grafting cross-linking percentage (GCP) and percentage grafting cross-linking efficiency (% GCE), were determined using Eqs. (1) and (2).

Grafting cross-linking percentage (GCP), is the weight ratio of grafted polymer to the original cellulose expressed as percentage. It indicates an increase in weight of the original cellulose subject to grafting with the monomer.

$$GCP = \left(\frac{W_g - W_c}{W_c}\right) \times 100 \tag{1}$$

Percentage grafting cross-linking efficiency (% GCE), is the fraction of synthetic polymer that is grafted onto cellulose in the total polymer expressed as percentage.

$$\%\, GCE = \left(\frac{W_g - W_c}{W_{cp} - W_c}\right) \times 100 \tag{2}$$

https://doi.org/10.1016/j.heliyon.2019.e01416

where W_g is the weight of the copolymer after extracting the homopolymer, W_c is the weight of cellulose used for the reaction and W_{cp} is the weight of the copolymer before extracting the homopolymer.

2.6.3. Swelling in water

A 0.1 g powdered PHG sample (250−350 μm) was weighed into a porous bag, immersed in distilled water and allowed to reach swelling equilibrium overnight at room temperature. The mass of the swollen PHG was determined after removing the surface water by gently dabbing with filter paper. The swelling ratio (water absorbency) at equilibrium (SEQ) was determined using Eq. (3) [3, 4].

$$SEQ = \left(\frac{M_{eq} - M_o}{M_o}\right) \tag{3}$$

where M_o (g) is the weight of dry PHG, M_{eq} (g) is the weight of swollen PHG and SEQ (g/g) is the swelling ratio at equilibrium.

2.6.4. FTIR spectroscopy

An FTIR spectrophotometer, Shimadzu IRAffinity-1S, was used to characterize the crude WH, isolated cellulose and cellulose-grafted PHG. The sample was finely ground, placed on the sample holder and pressed against the diamond and then scanned between 4000 cm^{-1} and 400 cm^{-1}.

2.6.5. Transmission electron microscopy

The morphology of copolymers was investigated using high resolution transmission electron microscope (HRTEM), Tecnai G2 F20 X-TWIN MAT instrumentation.

2.6.6. Swelling in salt solution

A 0.2 g powdered PHG sample was weighed into a porous bag and then immersed in different concentrations of NaCl, $CaCl_2$ and $AlCl_3$ solutions. It was left overnight at room temperature in order to achieve swelling equilibrium, weighed and water absorbency calculated using Eq. (3).

2.6.7. Influence of the pH on swelling

Several 0.2 g powdered PHG samples were weighed into porous bags and immersed in buffered solutions at different pH values. They were allowed to attain swelling equilibrium and then weighed. Potassium hydrogen phthalate, potassium dihydrogen phosphate and sodium tetraborate were used to prepare the buffer solutions, while HCl and NaOH were used to achieve the desired pH values.

https://doi.org/10.1016/j.heliyon.2019.e01416

2.6.8. Moisture holding capacity in soil

The method followed was adopted from Thombare *et al.* [26]. Soil sample was air-dried in the shade and passed through a 2 mm sieve. Sub-samples of air-dried soil weighing 100 g each were transferred into plastic beakers with perforations and filter paper lining at the base. The soil samples were then amended with 0.5, 1.0 and 1.5 g dry PHG (250−350 μm), while the untreated soil served as the control. The amendments were placed in a water tub and allowed to absorb water by capillarity for 12 h. They were then removed, allowed to drain excess gravitational water and kept under the same temperature and humidity. The weights of the moistened soil in the beakers were recorded at intervals of 2 days until there was no noticeable change. After subtracting the weight of the empty beaker and filter paper, the moisture holding capacity (MHC) of soil was calculated using Eq. (4).

$$MHC = \left(\frac{W_{wet} - W_{dry}}{W_{dry}}\right) \times 100 \tag{4}$$

where, W_{wet} is the weight of wet soil at a particular time and W_{dry} is the weight of air-dried soil.

2.6.9. Biodegradation of the PHG in soil

The method was adopted from Laftah and Hashim [3], where soil burial tests were used to simulate the natural degradation of PHG samples. Dry PHG samples (1 g each) of particle size $\leq$2 mm were placed in porous nylon bags that allowed the entry of micro-organisms and invertebrates. They were then buried in normal garden soil moistened to field capacity (30% w/w). Degradation was monitored through regular unearthing of the samples at 2-week intervals for a period of 14 weeks. The compost materials attached onto the surface of unearthed samples were removed, washed with distilled water and oven dried to constant weight at 60 °C. The percentage dry matter remaining at each sampling period was determined using Eq. (5).

$$Dry\ matter\ remaining\ (\%) = \left(\frac{W_t}{W_o}\right) \times 100 \tag{5}$$

where W_o is the initial weight of the sample and W_t is the weight of the sample after incubation time (t).

The decomposition rate constant (k) was determined using Olson single exponential model adopted by [26], Eq. (6).

$$W_t = W_o e^{-kt} \tag{6}$$

where W_o is the initial weight of the sample, W_t is the weight of the sample at incubation time t and k is the decomposition rate constant.

https://doi.org/10.1016/j.heliyon.2019.e01416

The half-life ($t_{1/2}$) was calculated using Eq. (7).

$$t_{1/2} = 0.693/k \quad (7)$$

2.6.10. Microbial culture and test for degradation of the copolymer

The methodology was adopted from Nawaz et al. [27, 28]. Acrylamide degrading microbes were isolated from the soil with history of exposure to alachlor (Roundup®), in a phosphate buffered medium (PBM) supplemented with 10 mM acrylamide. 5 soil samples were collected from randomly selected points in a coffee farm at the College of Agriculture and Veterinary Science, University of Nairobi. 5 g of each sample was placed in 250 mL conical flasks containing 50 mL PBM. This was covered with cotton wool and aluminum foil, and incubated for 10 days at 30 °C. 2 mL aliquot of microbial suspension was drawn from each of the flasks, transferred to a fresh 50 mL PBM (pH 7.5) and incubated for another 10 days. After 5 similar transfers, a 10 mL aliquot of each sample was centrifuged at 15,000 g × 10 min at 4 °C and the supernatant measured colorimetrically for liberated ammonia using indophenol blue method described by Hall [29]. Samples which tested positive for ammonia revealed acrylamide degradation. The pellet (microbial cells) was suspended in 10 mL PBM and after one wash; the suspension was sonicated for 5 min at intervals of 15 sec. At the same time, free NH_4^+ ions were leached out of the copolymers using distilled water and oven dried at 60 °C to a constant weight. 2 mL of microbial suspension was inoculated into a 100 mL PBM supplemented with 0.2−0.6 g of cellulose-grafted copolymer and copolymer without cellulose in separate flasks, then incubated at 30 °C. 10 mM acrylamide monomer and PBM without the substrate served as the reference and the blank, respectively. A 5 mL aliquot of the suspension was drawn at intervals of 20 h for 12 days, centrifuged and the supernatant tested for liberated ammonia.

2.7. Statistical data analysis

The data was subjected to ANOVA using IBM SPSS Statistics Version 20. Tukey honest significant difference (HSD) post hoc test was used to compare and assess the significance of the mean values at a probability level of $P \leq 0.05$.

3. Results and discussion

3.1. The composition of water hyacinth

The composition of air-dried WH is given in Table 1. Cellulose content ranged from 26.1 to 33.3 %, with the highest amount obtained from the stem, though not significantly different from the amount obtained from the leaves. The moisture content ranged from 9.2 to 9.3 %, ash from 13.0 to 24.1 %, hemicellulose from 16.1 to

https://doi.org/10.1016/j.heliyon.2019.e01416

Table 1. Composition of air-dried water hyacinth (%).

Plant part	Moisture	Ash	Hemicellulose	Lignin	Cellulose
Leaves	9.3 (0.21)^{a}	13.0 (0.10)^{a}	22.0 (0.45)^{c}	23.1 (0.25)^{b}	31.7 (0.25)^{bc}
Stem	9.3 (0.15)^{a}	20.2 (0.35)^{c}	16.1 (0.40)^{a}	20.8 (0.60)^{a}	33.3 (0.42)^{c}
Roots	9.3 (0.10)^{a}	24.1 (0.45)^{d}	19.7 (0.80)^{b}	20.6 (0.80)^{a}	26.1 (0.49)^{a}
Whole plant	9.2 (0.15)^{a}	18.4 (0.69)^{b}	20.8 (0.40)^{bc}	21.3 (0.26)^{a}	30.5 (1.30)^{b}

Note: The values in the parentheses are standard deviations (n = 3), different letters in the same column are significantly different (Tukey test; $P \leq 0.05$ level).

22.0 % and lignin from 20.6 to 23.1 %. No significant difference in the moisture content was observed amongst the plant parts. Significantly higher ash content ($P \leq 0.05$) was obtained in the roots, relative to the leaves and stem. Lignin and hemicellulose content was significantly higher ($P \leq 0.05$) in the leaves, compared to the stem and roots. The results are within the range of values obtained by other researchers. Girisuta *et al.* [30] reported 7.4 % moisture, 18.2 % ash, 47.7 % holocellulose (cellulose + hemicellulose) and 26.7 % lignin in leaves. Similarly, Reales-Alfaro *et al.* [31] characterized a 1:1 ratio of leaves to stem and reported 9.3 % moisture, 31.7% cellulose, 27.3 % hemicellulose and 3.9 % lignin. Saputra *et al.* [32] obtained values ranging from 8.3 to 9.2 % for moisture, 15.2−19.8 % ash, 62.2−64.2 % holocellulose and 7.3−10 % lignin in the stem. Mukaratirwa-Muchanyereyi *et al.* [33] reported 17.4−18.4 % ash and 17−23 % lignin in the roots. The slight variation in the composition may be attributed to the different methodologies used and the geographical location (source) of the WH.

The isolated cellulose fibres were dispersed in water due to the exposure of hydrophilic -OH groups; however, the dispersion (swelling) was irreversibly lost upon dehydration by either air- or oven-drying. This irreversible swelling probably relates to the collapse of spaces where hemicellulose and lignin were embedded leading to the restoration of strong inter- and intra-molecular H-bonds [5, 11]. The swelling of cellulose is a vital pre-condition to render the system accessible to the reagents. Bleaching with NaOCl decreases the crystallinity of cellulose, thus expanding the amorphous region where most grafting occurs [34]. Alkaline treatment loosens the inter-molecular interactions to allow the competing interactions with the swelling agent, *i.e.,* H_2O, where these interactions are restricted to the amorphous regions and pores [5, 11]. Consequently, the accessibility and reactivity of cellulose is improved in heterogeneous chemical reactions [11].

3.2. Mechanism of graft polymerization and extraction of homopolymers

Fig. 1 shows a possible mechanistic pathway for the synthesis of water hyacinth cellulose-graft-poly(ammonium acrylate-co-acrylic acid) PHG. The reaction is thought to initiate through thermal decomposition of APS to generate a sulphate

https://doi.org/10.1016/j.heliyon.2019.e01416

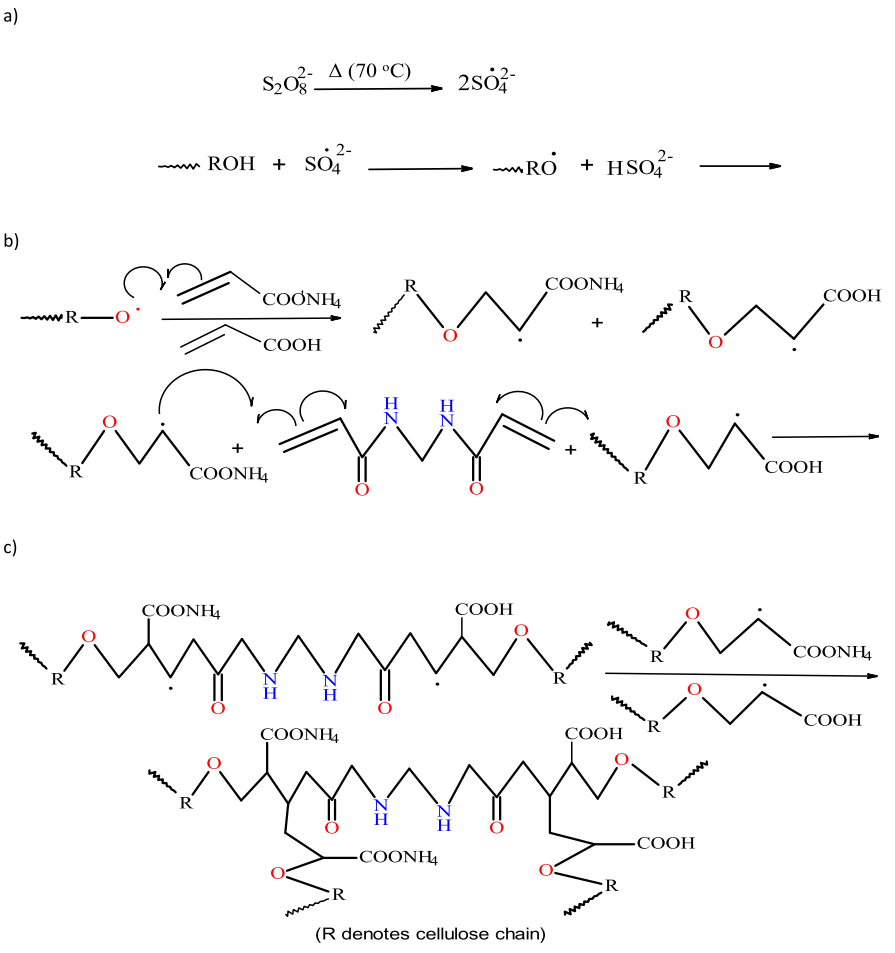

Fig. 1. Proposed mechanistic pathway for the synthesis of water hyacinth cellulose-g-poly(ammonium acrylate-co-acrylic acid) polymer hydrogel; a) thermal initiation, b) chain propagation and c) termination steps.

anion radical, which then abstracts H from an alcoholic −OH group in cellulose to form the corresponding macro-radical (Fig. 1a). Ammonium acrylate and acrylic acid (monomers) then become macro-radical receptors. The macro-radical initiated monomers in turn donate free radicals to the neighbouring molecules (chain propagation) (Fig. 1b) and subsequently, the grafting of the monomers onto cellulose chains leads to the formation of the graft copolymer. The chain terminates through combination of two growing polymer chains (Fig. 1c) [14].

The copolymer product was transformed from cellulose-g-poly(ammonium acrylate-co-acrylic acid) to cellulose-g-poly(acrylamide-co-acrylic acid) {cellulose-g-PAM-co-AA} upon heating (oven drying), according to Fig. 2.

The homopolymers were extracted from the graft copolymer using several solvents including; acetone, water, methanol, ethanol and an ethanol/acetone mixture. It was found that use of water alone takes long (about 3 days) while alcohol impacts

https://doi.org/10.1016/j.heliyon.2019.e01416

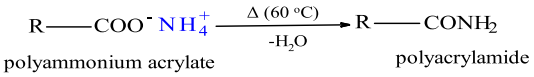

Fig. 2. Transformation of ammonium acrylate to acrylamide on heating (R denotes macro-molecule).

negatively on the hydrophilicity of the PHG material. Acetone was therefore adopted as the solvent of choice. Dehydration with ethanol or an ethanol/acetone mixture at normal temperatures generated heat, an indication of the formation of an exothermic chemical bond. It was likely that the un-neutralized acrylic acid (or ammonium acrylate) groups in the copolymer network caused the protonation of the -OH group in the alcohol, leading to the formation of an ester according to Fig. 3.

Fig. 4 shows photographs and high resolution transmission electron microscopy (TEM) images of oven-dried cellulose-g-PAM-co-AA and acetone-extracted cellulose-g-PAM-co-AA polymer hydrogels. Acetone did not influence the swelling property of PHG, and homopolymers were extracted effectively when dry PHG samples were swollen in water to enable the penetration of acetone. The acetone-extracted sample transformed from tough, brown solid material (Fig. 4a) to a white solid product (Fig. 4b), which could easily pulverize into fine powder. The white colour observed in Fig. 4(b) may be due to the micro-porous polymeric network structure. TEM micrographs of the oven-dried PHG showed a smooth dense material (Fig. 4c and d), whereas those of acetone-extracted PHG displayed foldings and voids which confirmed the presence of micro-pores (Fig. 4e and f). Acetone-extracted PHG samples were used in water absorption tests due to higher swelling ratio and faster swelling rate compared to the oven-dried PHG. Similar observations were made by Sannino *et al.* [13], who used a phase inversion desiccation technique in acetone to dehydrate a PHG based on sodium carboxymethyl cellulose and hydroxyethyl cellulose cross-linked with divinyl sulphone. The technique was found to induce a micro-porous structure into the PHG, which increased the water absorption and the swelling kinetics due to capillary effects.

3.3. Effect of the monomer to cross-linker ratio

The effect of the monomer to cross-linker ratio on GCP, % GCE and water absorbency of the PHG is shown in Table 2. In general, GCP, % GCE and water

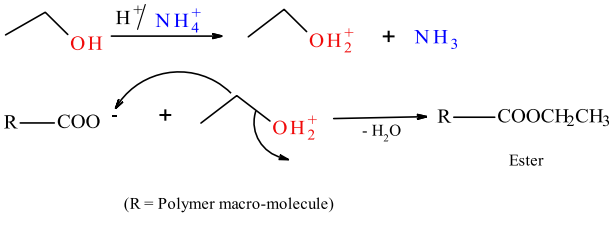

Fig. 3. Protonation of alcohol by un-neutralized acrylic acid or ammonium acrylate, leading to the formation of an ester.

https://doi.org/10.1016/j.heliyon.2019.e01416

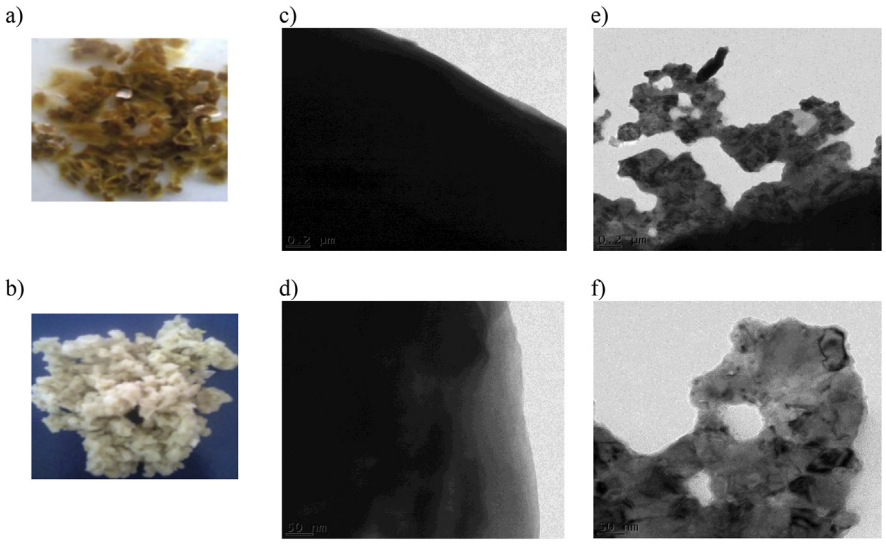

Fig. 4. Photographs of (a) oven-dried cellulose-g-PAM-co-AA, (b) acetone-extracted cellulose-g-PAM-co-AA; TEM images of (c & d) oven-dried cellulose-g-PAM-co-AA, (e & f) acetone-dehydrated cellulose-g-PAM-co-AA, at 0.2 μm and 50 nm scales.

absorbency all increased with increase in MBA and AA content. This observation may be attributed to the increased number of monomer molecules which increased the chances of collision with macro-radicals, resulting in improved grafting. However, optimum values of % GCE and water absorbency were observed at 6.75 % w/v AA content (highlighted in bold, Table 2). The observed increase in water

Table 2. Effect of AA and MBA ratio on GCP, % GCE and water Absorbency (SEQ).

Grafting parameter	AA content (% v/v)	MBA content (% w/v)				
		0.250	**0.375**	**0.500**	**0.625**	**0.750**
GCP	4.50	Weak	72 (6.0)	126 (5.1)	167 (5.0)	218 (11.0)
	5.75	174 (9.5)	214 (11.5)	253 (14.5)	302 (11.0)	346 (12.5)
	6.75	265 (12.6)	295 (12.0)	371 (16.0)	433 (12.6)	552 (17.5)
	7.75	290 (13.5)	333 (16.0)	413 (13.5)	458 (12.5)	567 (23.0)
	9.00	553 (21.5)	557 (20.5)	559 (23.5)	565 (24.5)	693 (22.0)
% GCE	4.50	Weak	41 (0.6)	68 (2.1)	78 (3.1)	83 (0.6)
	5.75	72 (2.5)	77 (2.6)	80 (3.5)	86 (1.0)	89 (2.0)
	6.75	**76 (2.4)**	**80 (2.5)**	**85 (3.6)**	**95 (2.1)**	**97 (1.0)**
	7.75	69 (3.5)	74 (1.6)	83 (3.0)	85 (2.5)	97 (2.5)
	9.00	52 (2.1)	58 (2.5)	60 (3.1)	74 (4.0)	82 (2.1)
SEQ	4.50	Weak	33 (3.1)	55 (2.1)	42 (1.5)	41 (4.4)
	5.75	99 (1.2)	104 (3.5)	100 (3.5)	85 (3.6)	69 (1.5)
	6.75	**142 (5.0)**	**151 (3.0)**	**156 (5.3)**	**139 (2.5)**	**95 (2.1)**
	7.75	139 (2.0)	145 (1.5)	107 (4.0)	98 (1.6)	79 (1.0)
	9.00	121 (3.5)	120 (2.2)	108 (3.6)	77 (2.7)	68 (2.6)

Notes: The values in parentheses are standard deviations (n = 3), reaction conditions; Degree of neutralization = 80 %, temp. = 80 °C, cellulose = 2 % w/v, APS = 0.25 % w/v, vol. = 40 mL, time = 2 h.

https://doi.org/10.1016/j.heliyon.2019.e01416

absorbency (SEQ) with increased AA content may be attributed to the increased density of hydrophilic groups in the copolymer network [2, 35]. The observed decrease in % GCE and SEQ at AA contents above the optimum could be attributed to favoured homopolymerization over graft polymerization, which led to poor grafting and subsequently, less hydrophilic copolymer with a loose network that could not effectively contain water molecules.

The SEQ increased with MBA content to an optimal value at 0.5 % w/v (Table 2), an observation that could be related to the monomer to cross-linker ratio which determines the cross-link density of the copolymer network [36, 37]. The increase in SEQ before the optimum MBA content was attributed to the low cross-link density and hydrophilicity of MBA which enhanced the swelling ratio of the copolymer [3, 36, 37]. On the other hand, the decrease in SEQ above the optimum MBA content may have resulted from a highly cross-linked network which decreased the porosity and flexibility of the polymer chains [3, 34]. Absorption of water is attributed to the balance between the osmotic and dispersive forces [34]. The osmotic force impels water molecules into the PHG, while the dispersive force exerted by the polymer chains resists it. The dispersive force increases with increased cross-link density hence, the observed decrease in water absorbency at high MBA content.

3.4. Effect of the degree of neutralization

The degree of neutralization (DN) is defined as the molar percentage of carboxyls in acrylic acid neutralized by a base, usually NaOH, KOH or NH_3 [36,38]. In this work, the carboxyl groups in acrylic acid were partially neutralized with NH_3. For a weak acid, the relationship between thepH and the dissociation equilibrium constant (K_a) is given by the well-known Henderson−Hasselbach Eq. (8).

$$pH = pK_a + \log\left[\frac{\alpha}{1-\alpha}\right] \tag{8}$$

where α is the DN. From the pK_a value of AA (4.25 at 25 °C) and the desired DN, the pH can be calculated.

The effect of DN on the GCP, % GCE and SEQ is shown in Table 3. The GCP and to some extent % GCE were found to decrease with increased DN, an observation attributed to the decreased cross-link density of the polymeric network. At low DN, the rate of polymerization is enhanced resulting in a high cross-link density and vice versa [36]. The SEQ was found to increase with increasing DN to an optimum value of 165 g/g at 70 % above which there was a decline. The initial increase could be attributed to decrease in cross-link density with increase in DN, whereas the decrease after the optimum could be due to weak network structure.

https://doi.org/10.1016/j.heliyon.2019.e01416

Table 3. Effect of degree of neutralization on GCP, %GCE and water absorbency.

Grafting parameter	Degree of neutralization (%)					
	40	**50**	**60**	**70**	**80**	**90**
GCP	331 (13.6)	322 (11.5)	304 (12.5)	293 (9.2)	281 (10.6)	271 (7.4)
% GCE	95 (1.2)	90 (2.2)	85 (2.4)	83 (2.6)	84 (2.3)	83 (2.6)
SEQ	108 (2.5)	123 (3.4)	142 (2.0)	**165 (4.2)**	158 (7.6)	112 (2.1)

Notes: The values in parentheses are standard deviations (n = 3), reaction conditions; AA = 6.75 % w/v, MBA = 0.5 % w/v, cellulose = 2 % w/v, APS = 0.25 % w/v, temp. = 80 °C, vol. = 40 mL, time = 2 h.

3.5. Effect of cellulose content and the total volume of the reaction mixture

The effect of cellulose content and the total volume of the reaction mixture on GCP, %GCE and SEQ are shown in Table 4. The GCP was found to decrease with increase in cellulose content and volume of the reaction mixture. The observation could be attributed to homopolymerization. Cellulose contents higher than the optimum favour homopolymer formation because the growing polymer chains are immobile and close to each other. At reaction volumes greater than the optimum, the macro-radicals are farther apart causing increased chain transfer reactions to monomer molecules and subsequently, a poorly grafted copolymer. The % GCE showed a general decrease with increased volume of the reaction mixture although some initial increase was observed at low cellulose contents, followed by a decline at higher cellulose contents. The SEQ was found to increase with increased cellulose content at a reaction volume of 40 mL to the optimum value of 165 g/g followed by a decline (highlighted in bold, Table 4). The observation could be attributed to well grafted copolymers and the hydrophilicity of cellulose. However, cellulose contents higher than the optimum value of 2.0 % w/v caused a decrease in SEQ due to the formation

Table 4. Effect of cellulose content and the volume of the reaction mixture on GCP, % GCE and water absorbency.

Grafting parameter	Reaction vol. (mL)	Amount of cellulose (%w/v)				
		1.50	**1.75**	**2.00**	**2.25**	**2.50**
GCP	40	454 (13.5)	343 (11.3)	306 (12.0)	263 (10.5)	237 (13.0)
	45	434 (9.6)	358 (12.5)	293 (11.3)	258 (11.5)	222 (10.0)
	50	396 (10.7)	296 (9.0)	236 (13.5)	203 (13.8)	203 (11.0)
%GCE	40	80 (1.4)	82 (2.5)	78 (1.7)	77 (2.1)	75 (3.0)
	45	81 (2.1)	78 (1.6)	76 (3.4)	72 (3.7)	66 (2.2)
	50	67 (3.1)	71 (2.0)	64 (2.7)	60 (3.5)	58 (3.1)
SEQ	40	**122 (4.9)**	**150 (5.4)**	**165 (4.0)**	**130 (1.5)**	**95 (1.0)**
	45	122 (2.5)	122 (3.0)	125 (2.1)	108 (4.0)	95 (2.1)
	50	103 (4.5)	107 (1.0)	104 (4.0)	104 (1.2)	101 (1.8)

Notes: The values in parentheses are standard deviations (n = 3), reaction conditions; AA = 6.75 % w/v, MBA = 0.5 % w/v, APS = 0.25 % w/v, temp. = 80 °C, time = 2 h.

https://doi.org/10.1016/j.heliyon.2019.e01416

of high number of physical entanglements, which acted as additional cross-link points. Mahfoudhi and Boufi [39] obtained comparable optimum SEQ values of 175, 152 and 145 g/g for cellulose nanofibrils (CNFs) contents of 3 %, 5 % and 10 % on assessing the effects of CNFs on the swelling properties of poly (acrylic acid-co-acrylamide)/CNFs nanocomposite PHG.

3.6. Effect of the initiator concentration

The effect of the initiator on GCP, % GCE and SEQ is shown in Table 5. The GCP was found to increase with increase in initiator concentration, an observation attributable to increased chances of H abstraction and chain transfer reaction between the monomers and cellulose macro-radicals. However, some decrease in % GCE was observed at high initiator content. This could be attributed to early termination of the growing polymer chains which lead to a poorly grafted copolymer. The SEQ increased to an optimum value of 165 g/g at 0.25 % w/v APS content, an observation which may be explained by the effect of initiator on the rate of polymerization and molecular weight distribution (MWD) of the copolymer [3, 12, 35, 36, 37]. Low initiator concentration lowers the rate of polymerization and increases MWD, and vice versa. At APS content lower than the optimum, the initiator is mostly utilized in the generation of macro-radical sites in cellulose where monomers can be grafted, resulting in improved SEQ. At APS content higher than the optimum, excess radicals may either lead to homopolymerization or termination through bi-molecular collisions, resulting in low MWD and loose network structure and thus, the observed decrease in the SEQ.

3.7. Effect of the reaction temperature

The effect of reaction temperature varaition on GCP % GCE and SEQ is shown in Table 6. The GCP and % GCE generally decreased with an increase in the reaction temperatures and the optimum SEQ was attained at 70 °C. The dependence of SEQ on the reaction temperature was attributed to the balance between chain growth, cross-linking and termination. Below the optimum, an increase in temperature could

Table 5. Effect of the initiator concentration on GCP, %GCE and water absorbency.

Grafting parameter	Amount of APS (%w/v)				
	0.125	**0.250**	**0.375**	**0.500**	**0.625**
GCP	287 (13.6)	305 (12.9)	336 (13.8)	328 (11.2)	353 (10.7)
% GCE	80 (2.6)	83 (1.8)	77 (3.7)	74 (5.1)	76 (2.9)
SEQ	113 (7.2)	**165 (5.0)**	131 (3.2)	111 (3.6)	107 (4.5)

Notes: The values in parentheses are standard deviations (n = 3), reaction conditions; AA = 6.75 % w/v, MBA = 0.5 % w/v, temp. = 80 °C, cellulose = 2%, vol. = 40 mL, time = 2 hr.

https://doi.org/10.1016/j.heliyon.2019.e01416

Table 6. Effect of the variation of reaction temperatures on GCP, %GCE and water absorbency.

Grafting parameter	Reaction temperature (°C)			
	50	60	70	80
GCP	380 (12.1)	320 (10.7)	308 (11.4)	345 (12.8)
% GCE	89 (2.8)	82 (3.1)	77 (3.5)	74 (2.4)
SEQ	113 (4.0)	140 (3.5)	165 (4.5)	150 (5.6)

Notes: The values in parentheses are standard deviations (n = 3), reaction conditions; AA = 6.75 % w/v, MBA = 0.5 % w/v, cellulose = 2%, APS = 0.25 % w/v, vol. = 40 mL, time = 2 hr.

have led to a predominant chain growth, whereas temperatures greater than the optimum may have led to a significant cross-linking and chain termination. High temperatures enhance not only the rate of decomposition of APS but also the kinetic energy of the radical centres and the diffusion of monomers into cellulose macroradicals [14]. However, temperatures higher than optimal may lead to a poorly grafted copolymer, a phenomenon attributed to: (a) increased rate of termination and chain transfer reactions to monomer molecules, and/or (b) decomposition of APS to yield O_2, a radical scavenger [12].

3.8. FTIR spectra of WH, isolated cellulose and cellulose-g-PAM-co-AA

Fig. 5 displays FTIR spectrum of WH, isolated cellulose and cellulose-g-PAM-co-AA, and the summary of the spectral bands is shown in Table 7. The spectral bands for both crude WH and purified cellulose were similar, except for a strong band at 1608.6 cm^{-1} assigned to the C=C stretch for the aromatic ring, which diminished in isolated cellulose. The delignification process removes lignin, a complex polymer derived from *p*-coumaryl, coniferyl and sinapyl alcohols coupled by aryl-ether bonds and ether cross-links. The intensity of the spectral bands at 1320-1210 cm^{-1} assigned to C-O stretch for alcohol and ether groups also decreased due to removal of lignin and hemicellulose. This indicates that lignin and hemicellulose were effectively removed. Grafting of the monomer onto cellulose was confirmed by comparing the FTIR spectrum of cellulose with that of cellulose-grafted PHG. The intense spectral band at 1018.4 cm^{-1} (Fig. 5a and b) assigned to the C-O stretch for primary or secondary alcohols was drastically weakened and shifted to 1029.9 cm^{-1} in cellulose-g-PAM-co-AA (Fig. 5c), implying that most of the -OH groups were involved in grafting. The spectrum of grafted cellulose also showed a broad band between 3700-2500 cm^{-1} assigned to N-H stretching and a strong band at 1541 cm^{-1} assigned to N-H bending for primary amides. These spectral bands are characteristic of the -$CONH_2$ group and hence confirmed the dehydration of ammonium acrylate to acrylamide upon oven drying at 60 °C. The broad band

https://doi.org/10.1016/j.heliyon.2019.e01416

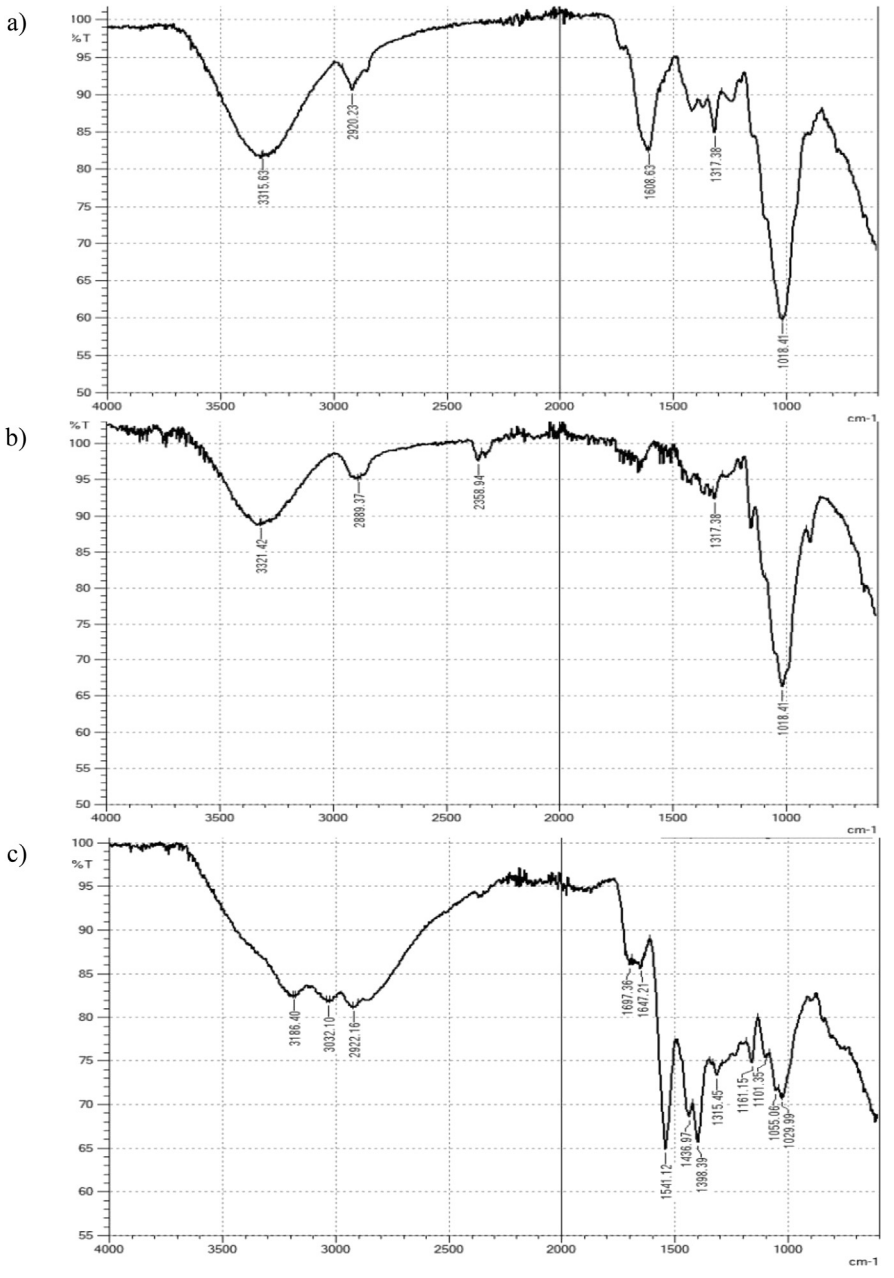

Fig. 5. FTIR spectra: a) crude water hyacinth, b) isolated cellulose, c) water hyacinth cellulose-g-PAM-co-AA.

extending from 3700-2500 cm^{-1} is also assigned to alcoholic and carboxylic −OH. The alcoholic -OH may be attributed to crystalline regions of cellulose that are unlikely to take part in grafting unless disrupted to allow penetration of monomers. The penetration of monomers is restricted to amorphous regions where most grafting occurs, though the reactivity of −OH under heterogeneous conditions may be influenced by steric effects from the chemical reagent and supra-molecular structure

https://doi.org/10.1016/j.heliyon.2019.e01416

Table 7. Summary of the spectral bands.

Wave number (cm^{-1})	Functional group
3700–3000	O-H stretch, alcohol
3700–2500	O-H stretch, carboxylic acid and alcohol N-H stretch, amide
2920, 2922, 2889	C-H stretch, SP^3 carbon
1647–1697	C=O stretch, amide
1608	C=C stretch, aromatic ring
1541	N-H bending, 1° amide
1440–1400	O-H bending, carboxylic acid
1320–1210	C-O stretch, alcohol, ether
1300–1000	C-O-C stretch, ether C-O stretch, alcohol, carboxylic acid
1018	C-O stretch, 1° or 2° alcohol

of cellulose [5, 11, 34]. The carboxylic −OH reveals the unneutralized portion of acrylic acid functional groups.

3.9. Influence of salt solutions on water absorbency

The effect of salt concentration and ionic charge on the SEQ is shown in Fig. 6a. The SEQ decreased in salt solutions, depending on the nature and the concentration of the metal cation, in the order; $Na^+ > Al^{3+} > Ca^{2+}$. This was attributed to lowering of the osmotic pressure, the driving force behind the swelling of the PHG [34, 40]. Furthermore, multivalent cations may have neutralized the charge at the surface of the PHG by complexing with carboxyamide and carboxylate groups leading to a highly cross-linked network with a small internal free volume [4, 41]. The SEQ was higher in the presence of trivalent Al^{3+} ions compared to divalent Ca^{2+} ions. The observation may be related to charge density, explained by increased electron pair attraction of strongly co-ordinated water molecules [41]. Small size and high charge density Al^{3+} ions bind water molecules strongly, co-ordinating them with the oxygen towards the cation and the hydrogens protruding. Due to electron cloud attraction by the cation, the H atoms of co-ordinated water molecules become more positive than bulk water molecules. Hence, they are more susceptible to formation of H-bonds with electron pairs of polymer dipolar groups such as carboxylic and amide oxygens. On the other hand, large and low charge density Ca^{2+} ions interfere with the water structure without creating an alternative radial structure [41]. Gupta and Shivakumar [40] observed a decrease in SEQ of poly(methacrylic acid-co-acrylamide) PHG from 155 to 30 g/g in aqueous solution containing Na^+ at concentrations ranging from 0.0001 to 1M, and also decreased SEQ with increased cationic charge in the order; $Na^+ > Ca^{2+} > Al^{3+}$, slightly different from the copolymer in the present study. The decrease was attributed to degree of cross-linking which

https://doi.org/10.1016/j.heliyon.2019.e01416

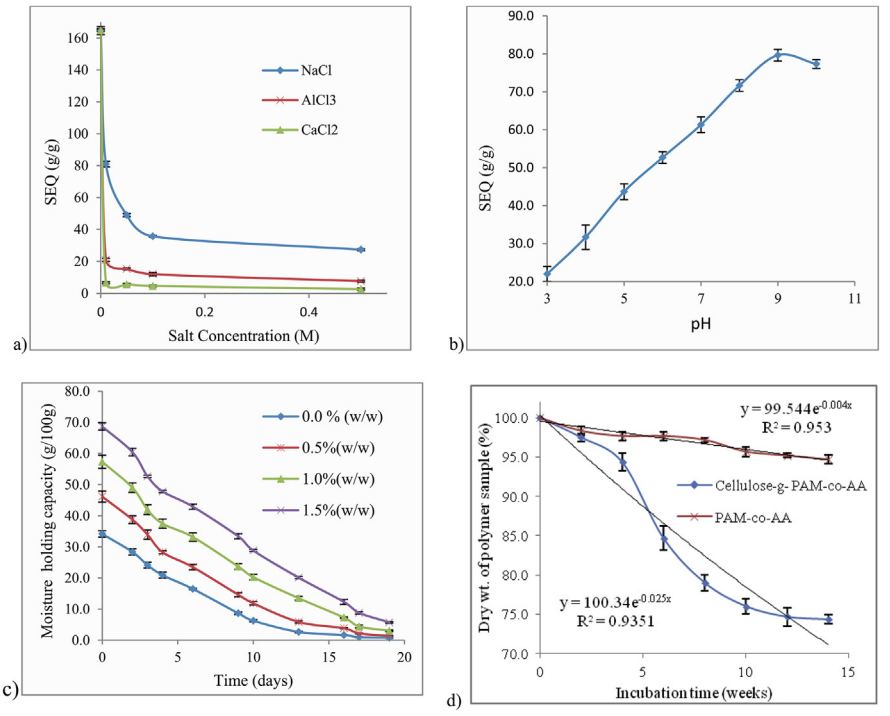

Fig. 6. a) Influence of salt concentration and ionic charge of the salt on the swelling of PHG, b) Influence of pH on the swelling of PHG, c) Moisture holding capacity of 100 g PHG-amended sandy-loam soil, d) Degradation curve of cellulose-grafted PHG and PHG without cellulose. Note: Results are reported as Mean ± SD (n = 3).

increased with cationic charge and the lowering of the pH of the swelling medium in the case of $AlCl_3$ salt. Shi *et al.* [4] also observed decreased SEQ values of guar gum-g-poly(sodium acrylate-co-styrene)/attapulgite PHG in the same order; $Na^+ > Ca^{2+} > Al^{3+}$, a phenomenon attributed to the "charge screening effect" and formation of chemical cross-links through complexation of carboxylate groups by multivalent cations.

3.10. Influence of pH on water absorbency

The effect of pH on SEQ of the hydrogel is shown in Fig. 6b. The SEQ values observed in buffer solutions ranged from 20 to 80 g/g, lower than values of 165 g/g and 120 g/g obtained in distilled and tap water, respectively. This indicates that the PHG was sensitive to charged species in the swelling medium. The SEQ increased with increase in pH of the solution, an observation attributable to the existence of ionizable (carboxyl) groups which present electrostatic repulsion to each other, expanding free volume to accommodate more water molecules [24]. However, excess NaOH may cause a "shielding effect" of Na^+ ions on the carboxylate by lowering the repulsion between them, hence decreasing the free volume. The low SEQ at low pH values relates to high proportion of undissociated -COOH groups

https://doi.org/10.1016/j.heliyon.2019.e01416

characterized by low degree of hydrophilicity and high ability to form H-bonds, resulting in a rigid network. Similar observations were made by Demitri *et al.* [15] who evaluated the swelling behaviour of sodium carboxymethyl cellulose/hydroxyethyl cellulose PHG at pH values ranging from 2 to 10. The SEQ increased from 37 to 95 g/g due to dissociation of -COOH groups, which depended on the pH of the swelling medium. Soleimani and Sadeghi [24] obtained a maximum SEQ value of 95 g/g at pH 8 in PHG based on starch-polyacrylate. Gupta and Shivakumar [40] obtained higher SEQ value of 160 g/g at pH 7.4. Mahfoudhi and Boufi [39] observed low SEQ in the pH range of 2−4, which increased from pH 5 to the maximum at pH 7, then declined thereafter.

3.11. Moisture holding capacity of PHG amended soil

Fig. 6c shows the moisture holding capacity (MHC) of sandy-loam soil amended with different amounts of PHG. The soil moisture contents of the amendments were recorded at an average temperature of 24 °C and humidity of 40. The initial values of the MHC were found to range from 35 % in the unamended soil to 68 % at 1.5 % (*w*/*w*) copolymer content. A gradual decrease in MHC was observed with time at different rates to near dryness as at 19^{th} day in all the amendments. Despite the factors that influence water absorbency such as soil pH and presence of cations, the copolymer revealed the capacity to absorb and retain moisture in soil. This is an important attribute for the efficient use of water in agriculture. The retention of moisture in soil is attributed to macro-molecular hindrance and hydrophilicity of the copolymer [15], which slows the release of absorbed water. In a similar study, Shahid *et al.* [42] obtained MHC values ranging from 35 to 65 % in sandy-loam soil amended with 0.1−0.4 % poly(acrylic acid-co-acrylamide)/AlZn-Fe_2O_4/K humate nanocomposite. The retention of moisture at relatively lower copolymer content was attributed to K humate which enhanced hydrophilicity. Thombare *et al.* [26] also obtained MHC values ranging from 39.8 to 51.57 % in sandy-loam soil amended with relatively lower copolymer content of 0.1−0.3 % guar gum based PHG. The MHC values were proportional to the amount of PHG added to the soil.

3.12. Biodegradation of cellulose grafted copolymer in soil

The degradation curves of cellulose-g-PAM-co-AA and PHG without cellulose are shown in Fig. 6d. Slow mass loss was observed in cellulose-grafted PHG in the first four weeks followed by a relatively faster loss from the 4^{th} to 12^{th} week, after which the curve tends to plateau. No considerable change in mass was observed in the case of PHG without cellulose. After 14 weeks, the mass loss was approximately 25 % for cellulose-g-PAM-co-AA and 5 % for PHG without cellulose. In a similar study, Laftah & Hashim [3] obtained a mass loss of about 9.6 % in cotton-g-poly(sodium acrylate-co-acrylic acid) PHG and 0.1 % in PHG without cotton after 14 weeks

https://doi.org/10.1016/j.heliyon.2019.e01416

incubation in soil. The lower mass loss relative to copolymers in the present study was attributed to highly crystalline cotton cellulose and stability of the copolymer. It follows that enhanced degradation of cellulose-g-PAM-co-AA is attributed to low degree of crystallinity of cellulose due to alkali treatment, in addition to amide-N that acted as source of nourishment to the microbes. The half-life ($t_{1/2}$) of cellulose-g-PAM-co-AA calculated from the rate constant of 0.025 week^{-1} (Fig. 6d) was found to be 27 weeks, significantly shorter than that of PAM-co-AA which was found to be 173 weeks. Thombare *et al.* [26] obtained a relatively higher degradation rate constant of 0.009 day^{-1} and $t_{1/2}$ of 77 days in guar gum-g-polyacrylic acid PHG cross-linked with di-methacrylic acid.

Fig. 7 shows swollen PHG before and after burying in moist soil. Cellulose-grafted PHG changed from whitish to dark-brown colour (Fig. 7a and b) after 14 weeks in moist soil. The brown colour of cellulose-grafted PHG (Fig. 7b) was darker than that of PHG without cellulose (Fig. 7c), an observation which may be revealing microbial degradation of copolymer chains. Oven-dried samples of unearthed cellulose-grafted PHG transformed from the initial tough solid (Fig. 4a) to a friable material, whereas PHG without cellulose remained tough. High molecular weight polymer chains are degraded by microbes into monomeric and oligomeric units to enable assimilation [43]. Native soil bacteria (*Pseudomonas, Xanthomonas, Rhodococcus, Klebseilla*) have been found to degrade and utilize polyacrylamide (PAM) as sole source of C and N under both aerobic and anaerobic conditions [27, 28, 43, 44]. They secrete PAM-specific extracellular *amidase* (*amidohydrolase*) enzyme to hydrolyse the amide group into acrylic acid and ammonia, according to Fig. 8. Acrylic acid is eventually degraded to carbon dioxide and water. The addition of C sources into PAM has been reported to promote bacterial growth; Yu *et al.* [43] observed improved degradation efficiency of PAM in culture medium supplemented with glucose. In this case, the grafted cellulose could have enhanced the degradation of the copolymer.

3.13. Degradation of the copolymer by soil microbial isolates

Of the 5 soil samples incubated in phosphate buffered medium (PBM) supplemented with acrylamide, 3 tested positive for NH_4^+. Acrylamide degrading microbes have

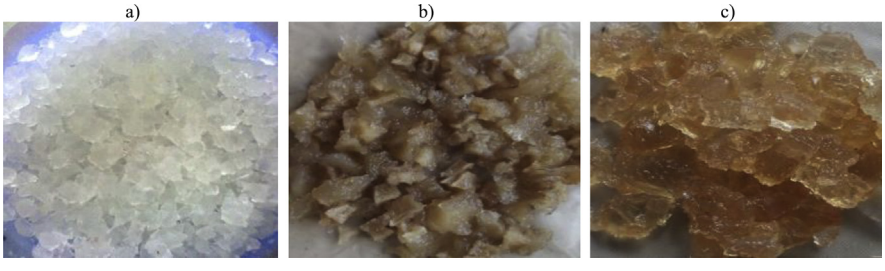

Fig. 7. a) swollen cellulose-g-PAM-co-AA before burying in moist soil, b) swollen cellulose-g-PAM-co-AA after 14 weeks in moist soil, c) swollen PHG without cellulose after 14 weeks in moist soil.

https://doi.org/10.1016/j.heliyon.2019.e01416

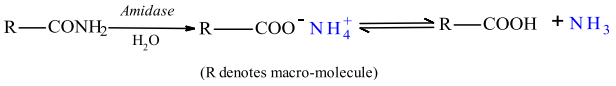

Fig. 8. Enzymatic hydrolysis of acrylamide to carboxylic acid and ammonia.

been reported in soil contaminated with amides and their derivatives such as herbicides [45]. These microbes transform herbicides such as propanil (acrylamilide) to amides and eventually NH_4^+, to support their growth [45]. They have been isolated, identified and the *amidase* enzyme purified and characterized [27, 28, 43, 44]. The present study focused on utilizing the soil microbial isolates to degrade acrylamide copolymers; therefore, the microbes involved could be more than one species.

Table 8 shows the amount of NH_4^+ liberated with time in PBM supplemented with acrylamide and different amounts of the copolymer as the sole source of C and N. The amount of NH_4^+ accumulated in the copolymer supplemented media increased with time to maximum values at 100 h above which some decline were observed. The decrease after the maxima may be attributed to utilization of NH_4^+ by the microbes as N source. The amount of NH_4^+ accumulated in the media for both

Table 8. Concentration of NH_4^+ (mg/kg) liberated with time (hours) at different copolymer contents.

Sample code	6 h	20 h	40 h	60 h	80 h	100 h	168 h	216 h	288 h
AM	0.5 (0.1)	1.1 (0.1)	1.5 (0.3)	1.9 (0.2)	20.9 (2.0)	54.8 (1.9)	95.8 (3.3)	112.2 (4.2)	93.9 (3.0)
P1	6.7 (1.6)^{a}	11.1 (0.2)^{a}	19.4 (1.4)^{a}	17.4 (1.0)^{a}	20.9 (1.9)^{a}	34.6 (1.6)^{a}	21.7 (2.4)^{a}	21.1 (1.2)^{a}	22.7 (0.6)^{a}
P2	10.6 (2.3)^{ab}	14.7 (1.5)^{ab}	31.6 (2.4)^{b}	26.4 (1.8)^{b}	37.8 (0.4)^{c}	50.4 (2.2)^{c}	33.8 (2.9)^{a}	33.8 (1.7)^{b}	34.3 (3.1)^{b}
P3	11.7 (2.5)^{b}	22.2 (2.8)^{cd}	41.6 (1.7)^{c}	56.0 (0.9)^{d}	62.8 (1.4)^{e}	66.9 (0.5)^{d}	63.3 (1.6)^{bc}	67.2 (7.4)^{d}	64.1 (1.0)^{de}
P4	12.3 (1.6)^{b}	28.3 (1.7)^{d}	56.9 (1.5)^{cd}	61.9 (2.6)^{e}	64.3 (0.8)^{e}	80.3 (1.9)^{e}	80.3 (3.2)^{d}	64.3 (0.6)^{d}	52.3 (2.1)^{c}
CP1	12.8 (1.7)^{b}	13.3 (0.5)^{ab}	30.6 (2.4)^{b}	24.1 (1.5)^{b}	34.3 (1.5)^{b}	42.0 (3.7)^{b}	27.7 (3.8)^{a}	28.3 (1.0)^{ab}	32.3 (3.2)^{b}
CP2	13.9 (1.2)^{b}	19.2 (1.0)^{bc}	41.8 (1.6)^{c}	38.9 (1.8)^{c}	47.0 (1.0)^{d}	60.7 (1.8)^{d}	53.3 (2.0)^{b}	49.8 (2.6)^{c}	56.3 (3.2)^{cd}
CP3	13.5 (1.9)^{b}	21.1 (2.4)^{c}	56.1 (2.1)^{d}	51.8 (2.0)^{d}	64.6 (0.5)^{e}	81.1 (2.5)^{e}	57.4 (10.3)^{bc}	58.2 (0.8)^{cd}	61.7 (3.8)^{de}
CP4	14.1 (1.9)^{b}	20.7 (3.3)^{c}	52.5 (2.0)^{d}	53.9 (0.8)^{d}	63.3 (1.6)^{e}	81.7 (2.5)^{e}	68.0 (3.7)^{cd}	66.6 (4.6)^{d}	65.6 (3.4)^{e}

Notes: The values in parentheses are standard deviations (n = 3), different letters in the same column are significantly different (Tukey test; $P \leq 0.05$ level).
Key: AM = Acrylamide monomer, 10 mM {0.07 % (w/v)}, P = PAM-co-AA; P1 = 0.02, P2 = 0.04, P3 = 0.05 & P4 = 0.06 (%w/v), CP = Cellulose-g-PAM-co-AA; CP1 = 0.02, CP2 = 0.04, CP3 = 0.05 & CP4 = 0.06 % (w/v).

https://doi.org/10.1016/j.heliyon.2019.e01416

copolymers increased significantly ($p \leq 0.05$) with the copolymer content (P1 to P3 & CP1 to CP3) from 40 to 100 h. The values recorded in 0.05 % (w/v) copolymer content (P3 & CP3) were in most instances, not significantly different from those observed in 0.06 % (w/v) (P4 & CP4). Significantly higher accumulation of NH_4^+ was observed in the cellulose grafted copolymer CP1 and CP2 from 40 to 100 h, relative to similar content of the copolymer without cellulose P1 and P2. The observation may be attributed to easily accessible cellulose-C which enhanced microbial growth and subsequently, increased amount of enzyme that caused considerable hydrolysis of the amide-N.

The degradation of the copolymers was not compared statistically with that of acrylamide (monomer) due to cross-linked network which must be degraded into monomeric units to enable microbial assimilation. Acrylamide supplemented medium showed low content of NH_4^+ ranging from 1.1 to 1.9 mg/kg in the first 60 h, reflecting the lag phase, which then increased considerably from 20 mg/kg at 80 h to a maximum value of 112.2 mg/kg at 216 h above which it declined. In related studies on the degradation of acrylamide by *Pseudomonas sp.,* Shanker *et al.* [44] observed the highest accumulation of NH_4^+ after 6 days, at 30 °C. Nawaz *et al.* [27] using *Pseudomonas sp.,* observed maximum NH_4^+ content after 24 h, at 28 °C which decreased to 1.0 mM at 96 h; whereas, *Xanthomonas maltophilia* showed the highest accumulation of NH_4^+ and acrylic acid at 48 h under the same conditions. In both cases, the highest acrylic acid content coincided with the disappearance of acrylamide and decreased with cellular growth. Nawaz *et al.* [28] in degradation of 62 mM acrylamide by *Rhodococcus sp.,* observed maximum accumulation of NH_4^+ and acrylic acid after 24 h and a peak cellular growth from 72 to 96 h at 28 °C. The variation in the time taken to achieve maximum NH_4^+ accumulation between the present and previous studies on the acrylamide may be related to the microbial (bacterial) species involved in the degradation and the initial population of microbes in the culture media.

The present study revealed hydrolysis of amide-N by soil microbial isolates. The potential agricultural application of the cellulose grafted copolymer in the formulation of slow release fertilizer was carried out in a separate study [46]. The results of the study revealed contribution of hydrolyzed amide-N to mineral-N content in the soil.

4. Conclusion

Acrylic monomers have been grafted onto swollen cellulose isolated from water hyacinth by radical polymerization to form cellulose-g-PAM-co-AA polymer hydrogel. The influence of reaction conditions on grafting was assessed using grafting parameters, namely, GCP, % GCE and water absorption. FTIR spectra revealed purification of cellulose from WH and grafting of the monomer onto the cellulose. High

https://doi.org/10.1016/j.heliyon.2019.e01416

resolution TEM images displayed a micro-porous structure in acetone-dehydrated PHG. The optimized product was obtained at 6.5 % w/v AA content, 0.5 % w/v MBA content, 70 % degree of neutralization, a reaction volume of 40 mL, 2 % cellulose content and a temperature of 70 °C. The highest water absorbency in distilled water was found to be 165 g/g, and the swelling was influenced by the presence, concentration and nature of ions present. The cellulose grafted copolymer revealed significant hydrolysis of amide-N in the microbial culture, displayed biodegradability and the potential to absorb and retain water in the soil. These are important features for potential agricultural applications such as formulation of slow release fertilizers and soil conditioning.

Declarations

Author contribution statement

Kiplangat Rop: Conceived and designed the experiments; Performed the experiments; Analyzed and interpreted the data; Contributed reagents, materials, analysis tools or data; Wrote the paper.

Damaris Mbui: Conceived and designed the experiments; Analyzed and interpreted the data; Contributed reagents, materials, analysis tools or data.

Njagi Njomo, George N. Karuku, Immaculate Michira: Analyzed and interpreted the data; Contributed reagents, materials, analysis tools or data.

Rachel F. Ajayi: Contributed reagents, materials, analysis tools or data.

Funding statement

This work was supported by DAAD scholarship award and National Research Fund of Kenya.

Competing interest statement

The authors declare no conflict of interest.

Additional information

No additional information is available for this paper.

Acknowledgements

The authors acknowledge University of Nairobi staff, Mr. Evans Kimega, Mr. Edwin Rono and Ms. Rose Mutungi for their technical assistance.

https://doi.org/10.1016/j.heliyon.2019.e01416

References

[1] E.M. Ahmed, Hydrogel: preparation, characterization and applications: a review, J. Adv. Res. 6 (2015) 105−121.

[2] Y. Yu, L. Liu, Y. Kong, E. Zhang, Y. Liu, Synthesis and properties of N-maleyl chitosan cross-linked poly(acrylic acid-co-acrylamide) superabsorbents, J. Polym. Environ. 19 (2011) 926−934.

[3] W. Laftah, S. Hashim, Synthesis, optimization, characterization and potential agricultural application of polymer hydrogel composites based on cotton microfiber, Chem. Pap. 68 (2014) 798−808.

[4] X.N. Shi, W.B. Wen, A.Q. Wang, Effect of surfactant on porosity and swelling behaviors of guar gum-g-poly(sodium acrylate-co-styrene)/attapulgite superabsorbent hydrogels, Coll. Surf. B Biointer. 88 (2011) 279−286.

[5] D. Roy, M. Semsarilar, J.T. Guthriea, S. Perrier, Cellulose modification by polymer grafting: a review, RSC Chem. Soc. Rev. 38 (2009) 1825−2148.

[6] A. Sannino, C. Demitri, M. Madaghiele, Biodegradable cellulose-based hydrogels: design and applications: a review, Materials 2 (2009) 353−373.

[7] X. Qiu, S. Hu, "Smart" materials based on cellulose: a review of the preparations, properties, and application, Materials 6 (2013) 738−781.

[8] A. Carlmark, E. Larsson, E. Malmstrom, Grafting of cellulose by ring-opening polymerization: a review, Eur. Polym. J. 48 (2012) 1646−1659.

[9] E. Malmström, A. Carlmark, Controlled grafting of cellulose fibres − an outlook beyond paper and cardboard, Polym. Chem. 3 (2012) 1702−1713.

[10] W.A. Laftah, S. Hashim, A.N. Ibrahim, Polymer hydrogels: a review, Polym. Plast. Technol. Eng. 50 (2011) 1475−1486.

[11] R. Pönni, Changes in accessibility of cellulose for kraft pulps measured by deuterium exchange, Aalto Univ. Doc. Dissert. 68 (2014).

[12] M. Sadeghi, S. Safari, H. Shahsavari, H. Sadeghi, F. Soleimani, Effective parameters onto graft copolymer based on carboxymethyl with acrylic monomer, Asian J. Chem. 25 (2013) 5029−5032.

[13] A. Sannino, G. Mensitieri, L. Nicolais, Water and synthetic urine sorption capacity of cellulose based hydrogels under a compressive stress field, J. Appl. Polym. Sci. 91 (2004) 3791−3796.

https://doi.org/10.1016/j.heliyon.2019.e01416

[14] M. Sadeghi, F. Soleimani, M. Yarahmadi, Chemical modification of carboxymethyl cellulose via graft copolymerization and determination of the grafting parameters, Orient. J. Chem. 27 (2011) 967–972.

[15] C. Demitri, F. Scalera, M. Madaghiele, A. Sannino, A. Maffezzoli, Potential of cellulose-based superabsorbent hydrogels as water reservoir in agriculture, Int. J. Polym. Sci. (2013).

[16] N. Jafari, Ecological and socio-economic utilization of water hyacinth, *Eichhornia crassipes*, J. Appl. Sci. Environ. Manag. 14 (2010) 43–49.

[17] T. Istirokhatun, N. Rokhati, R. Rachmawaty, M. Meriyani, S. Priyanto, H. Susanto, Cellulose isolation from tropical water hyacinth for membrane preparation, Proc. Environ. Sci. 23 (2015) 274–281.

[18] Y.L. Zhu, A.M. Zayed, J.H. Qian, M. de Souza, N. Terry, Phytoaccumulation of trace elements by wetland plants: II. Water hyacinth, J. Environ. Qual. 28 (1999) 339–344.

[19] A. Kivaisi, M. Mtila, Production of biogas from water hyacinth (*Eichhornia crassipes*) (Mart) (Solms) in a two-stage bioreactor, World J. Microbiol. Biotechnol. 14 (1997) 125–131.

[20] U.S. Aswathy, R.K. Sukumaran, G.L. Devi, K.P. Rajasree, R.R. Singhania, A. Pandey, Bio-ethanol from water hyacinth biomass: an evaluation of enzymatic saccharification strategy, Bioresour. Technol. 101 (2010) 925–930.

[21] S. Rezania, M.F. Din, S.F. Kamaruddin, S.M. Taib, L. Singh, E.L. Yong, A.F. Dahalan, Evaluation of water hyacinth (*Eichhornia crassipes*) as a potential raw material source for briquette production, Energy 111 (2016) 768–773.

[22] E.S. Abdel-Halim, Chemical modification of cellulose extracted from sugarcane bagasse: preparation of hydroxyethyl cellulose, Arab. J. Chem. 7 (2014) 362–371.

[23] H. Kaco, S. Zakaria, N.F. Razali, C.H. Chia, L. Zhang, S.M. Sani, Properties of cellulose hydrogel from kenaf core prepared via pre-cooled dissolving method, Sains Malays. 43 (2014) 1221–1229.

[24] F. Soleimani, M. Sadeghi, Synthesis of pH-sensitive hydrogel based on starch-polyacrylate superabsorbent, J. Biomater. Nanobiotechnol. 3 (2012) 310–331.

[25] G. Gürdağ, S. Sarmad, Cellulose graft copolymers: synthesis, properties and applications, in: S. Kalia, M. Sabaa (Eds.), Polysaccharide Based Graft Copolymers, Berlin, Heidelberg, 2013, pp. 15–57.

https://doi.org/10.1016/j.heliyon.2019.e01416

[26] N. Thombare, S. Mishra, M.Z. Siddiqui, U. Jha, D. Singh, G.R. Mahajan, Design and development of guar gum based novel, superabsorbent and moisture retaining hydrogels for agricultural applications, Carbohy. Polym. 185 (2018) 169−178.

[27] M.S. Nawaz, W. Franklin, C.E. Cerniglia, Degradation of acrylamide by immobilized cells of a *Pseudomonas sp*. and *Xanthomonas maltophilia*, Can. J. Microbiol. 39 (1993) 207−212.

[28] M.S. Nawaz, A.A. Khan, J.E. Seng, J.E. Leakey, P.H. Siitonen, C.E. Cerniglial, Purification and characterization of an amidase from an acrylamide-degrading *Rhodococcus sp*, Appl. Environ. Microbiol. 60 (9) (1994) 3343−3348.

[29] A. Hall, Application of the indophenol blue method to the determination of ammonium in silicate rocks and minerals, Appl. Geochem. 8 (1993) 101−105.

[30] B. Girisuta, B. Danon, R. Manurung, L. Janssen, H. Heeres, Experimental and kinetic modelling studies on the acid-catalysed hydrolysis of the water hyacinth plant to levulinic acid, Bioresour. Technol. 99 (2008) 8367−8375.

[31] J.G. Reales-Alfaro, L.T. Trujillo-Daza, G. Arzuaga-Lindado, H.I. Castaño-Peláez, A.D. Polo-Córdoba, Acid hydrolysis of water hyacinth to obtain fermentable sugars, Cienc. Tecnol. Futuro 5 (2013) 101−112. Retrieved March 02, 2019, from, http://www.scielo.org.co/scielo.php?script=sci_arttext&pid=S0122-53832013000100008&lng=en&tlng=en.

[32] A.H. Saputra, M. Hapsari, A.B. Pitaloka, Synthesis and characterization of CMC from water hyacinth cellulose using isobutyl-isopropyl alcohol mixtures as reaction medium, Contemp. Eng. Sci. 8 (2015) 1571−1582.

[33] N. Mukaratirwa-Muchanyereyi, J. Kugara, M.F. Zaranyinka, Surface composition and surface properties of water hyacinth (*Eichhonia crassipes*) root biomass: effect of mineral acid and organic solvent treatments, Afr. J. Biotechnol. 15 (2016) 897−909.

[34] D. Swantomo, R. Rochmadi, K.T. Basuki, R. Sudiyo, Synthesis and characterization of graft copolymer rice straw cellulose-acrylamide hydrogels using gamma irradiation, Atom Indones. 39 (2013) 57−62.

[35] M. Sadeghi, M. Yarahmadi, Synthesis and properties of biopolymer based on carboxymethyl cellulose-g-poly(N-vinyl pyrollidin-co-2-acrylamido-2-methyl propan sulfonic acid as superabsorbent hydrogels, Orient. J. Chem. 27 (1) (2011) 13−21.

https://doi.org/10.1016/j.heliyon.2019.e01416

[36] M. Liu, R. Liang, F. Zhan, Z. Liu, A. Niu, Preparation of superabsorbent slow release nitrogen fertilizer by inverse suspension polymerization, Polym. Int. 56 (2007) 729−737.

[37] A. Li, R. Liu, A. Wang, Preparation of starch-graft-poly(acrylamide)/attapulgite superabsorbent composite, J. Appl. Polym. Sci. 98 (2005) 1351−1357.

[38] M. Guo, M. Liu, Z. Hu, F. Zang, L. Wu, Preparation and properties of a slow release NP compound fertilizer with superabsorbent and moisture preservation, J. Appl. Polym. Sci. 96 (2005) 2132−2138.

[39] N. Mahfoudhi, S. Boufi, Poly(acrylic acid-co-acrylamide)/cellulose nanofibrils nanocomposite hydrogels: effects of CNFs content on the hydrogel, Cellulose 23 (2016) 3691−3701.

[40] N.V. Gupta, H.G. Shivankumar, Investigation of swelling behaviour and mechanical properties of a pH sensitive superporous hydrogel composite, Iran. J. Pharm. Res. 11 (2012) 481−493.

[41] Y.D. Livney, I. Portnaya, B. Faupin, O. Ramon, Y. Cohen, U. Cogan, S. Mizrahi, Interactions between inorganic salts and polyacrylamide in aqueous solutions and gels, J. Polym. Sci. B Polym. Phys. 41 (2003) 508−519.

[42] S.A. Shahid, A.A. Qidwai, F. Anwar, I. Ullah, U. Rashid, Effects of a novel poly(AA-co-AAm)/AlZnFe2O4/potassium humate superabsorbent hydrogel nanocomposite on water retention of sandy loam soil and wheat seedling growth, Molecules 17 (2012) 12587−12602.

[43] F. Yu, R. Fu, Y. Xie, W. Chen, Isolation of polyacrylamide-degrading bacteria from dewatered sludge, Int. J. Environ. Res. Public Health 12 (2015) 4214−4230.

[44] R. Shanker, C. Ramakrishna, P.K. Seth, Microbial degradation of acrylamide monomer, Arch. Microbiol. 154 (1990) 192−198.

[45] M.S. Nawaz, W. Franklin, W.L. Campbell, T.M. Heinze, C.E. Cerniglia, Metabolism of acrylonitrile by *Klebseilla pneumonia*, Arch. Microbiol. 156 (1991) 231−238.

[46] K. Rop, G.N. Karuku, D. Mbui, I. Michira, N. Njomo, Formulation of slow release NPK fertilizer (cellulose-graft-poly (acrylamide)/nano-hydroxyapatite/soluble fertilizer) composite and evaluating its N mineralization potential, Annal. Agric. Sci. 63 (2018) 163−172.

https://doi.org/10.1016/j.heliyon.2019.e01416